

Tough and Sustainable Graft Block Copolymer Thermoplastics

Jiuyang Zhang,[†] Tuoqi Li,[†] Alexander M. Mannion,[†] Deborah K. Schneiderman,[‡] Marc A. Hillmyer,[‡] and Frank S. Bates*

[†]Department of Chemical Engineering and Materials Science and [‡]Department of Chemistry, University of Minnesota, Minneapolis, Minnesota 55455-0431, United States

Supporting Information

ABSTRACT: Fully sustainable poly[HPMC-g-(PMVL-b-PLLA)] graft block copolymer thermoplastics were prepared from hydroxypropyl methylcellulose (HPMC), β -methyl- δ -valerolactone (MVL), and L-lactide (LLA) using a facile two-step sequential addition approach. In these materials, rubbery PMVL functions as a bridge between the semirigid HPMC backbone and the hard PLLA end blocks. This specific arrangement facilitates PLLA crystallization, which induces microphase separation and



HPMC-q-[PMVL-b-PLLA] = Tough Plastics

physical cross-linking. By changing the backbone molar mass or side chain composition, these thermoplastic materials can be easily tailored to access either plastic or elastomeric behavior. Moreover, the graft block architecture can be utilized to overcome the processing limitations inherent to linear block polymers. Good control over molar mass and composition enables the deliberate design of HPMC-g-(PMVL-b-PLLA) samples that are incapable of microphase separation in the melt state. These materials are characterized by relatively low zero shear viscosities in the melt state, an indication of easy processability. The simple and scalable synthetic procedure, use of inexpensive and renewable precursors, and exceptional rheological and mechanical properties make HPMC-g-(PMVL-b-PLLA) polymers attractive for a broad range of applications.

hermoplastics are versatile and melt processable materials used in a wide range of products including packaging, 1,2 medical equipment, 1,3 and textiles. 2,4 One important subclass of thermoplastics is linear triblock polymers consisting of a rubbery midblock anchored by two hard end blocks that microphase separate into discrete domains. 5,6 These linear triblock polymers can achieve desirable mechanical properties in both the elastomeric and plastic limit based on judicious choice of polymer molar mass and composition. 5,7,8' Because the order-disorder transition temperatures (T_{ODT}) of linear triblocks scale with the overall molecular weight, high molar mass triblocks are often not amenable to high shear melt processing. Contrarily, linear $(AB)_n$ multiblock polymers have shown considerable promise for their ability to decouple the T_{ODT} from total molar mass.

Multiblock materials are also appealing for their dramatically enhanced mechanical properties, particularly in the plastic limit. 5,7,10-12 The impressive toughness of linear multiblocks has been attributed to the presence of interior blocks, which bridge individual microdomains and increase the overall connectivity of the physically cross-linked material. 7,10,13 However, this architecture also has some inherent disadvantages. The mobility of the interior segments is limited; consequently, multiblock copolymers theoretically capable of crystallization (e.g., those containing isotactic poly(L-lactide) (PLLA) blocks) may exhibit low crystallinity and a decreased upper use temperature relative to the linear triblock. 10 Additionally, because molar mass and melt viscosity are correlated, linear multiblock polymers can be difficult to process even in the disordered state. 14,15

To overcome these disadvantages, more complex molecular architectures may be utilized, such as star polymers and graft polymers. 16-20 Branched structures such as these tend to have lower viscosities at high shear rates and improved processability compared to linear chains with similar molar mass.²¹ Of the numerous possible branched structures, the graft polymer architecture is particularly attractive because of its intrinsic tunability. Varying the backbone length and the size, composition, and density of the grafted chains will influence the rheological and mechanical properties.²² In the past few decades, graft polymers have attracted increasing attention for use as thermoplastics. 18

Weidisch and co-workers, for example, prepared block copolymers containing a rubbery polyisoprene backbone with glassy polystyrene grafts and reported excellent thermoplastic properties. 20,23 In other studies, acrylic-based random copolymers and polylactide homopolymers have been grafted from rigid cellulosic backbone chains.^{24–26} Although these graft polymers show promise as potentially versatile materials, previous investigations have focused almost exclusively on graft polymers with homopolymer or random copolymer grafts. The utilization of graft block polymers as thermoplastics has been far less investigated.

We hypothesized that a graft block architecture—specifically one where amorphous rubbery segments are used to tether hard end blocks to a semirigid backbone—could be used to

Received: February 1, 2016 Accepted: February 29, 2016 Published: March 4, 2016

ACS Macro Letters Letter

Scheme 1. Synthetic Route for HPMC-g-(PMVL-b-PLLA)^a

"R in the scheme represents -H, -Me, or $-CH_2CH(OH)CH_3$ as the substituted group of HPMCs. In this work, we designate polymers with HPMC (a, x) to represent HPMC-g-(PMVL-b-PLLA), where "a" designates the molecular weight (M_n) of the side-chain, PMVL, in kg/mol and "x" is the volume fraction of PLLA.

Table 1. Composition and Thermal Characteristics of HPMC-g-PMVL Homopolymers and HPMC-g-(PMVL-b-PLLA) Graft Copolymers

samples	$^{a}M_{n}$ (kg/mol)	${}^{\boldsymbol{b}}\!f_{\mathrm{L}}$	c $\! D$	$^{d}T_{g,M}$ (°C)	$^{d}T_{g,L}$ (°C)	^e X (%)	f_{T_m} (°C)
HPMC15-g-PMVL	650	-	1.86	-53	-	-	-
HPMC15 (8.5, 0.3)	950	0.31	1.50	-42	31	10	143
HPMC15 (8.5, 0.5)	1350	0.48	1.60	-41	51	9	159
HPMC15 (8.5, 0.7)	2260	0.69	-	-42	57	11	169
HPMC40 (8.1, 0.7)	5140	0.70	-	-41	58	10	168
LML (26, 0.3)	38	0.28	1.10	-44	53	22	161

"Number-average molecular weight based on ¹H NMR analysis of graft chain composition (ratio of end groups to repeat units) and the estimated number of grafts per HPMC backbone (see SI for details regarding this calculation). ^bVolume fraction of PLLA determined by ¹H NMR and calculated based on published bulk homopolymer room-temperature densities. ⁷ ^cDispersity (D) measured by SEC. HPMC15 (8.5, 0.7) and HPMC40 (8.1, 0.7) could not pass through the SEC columns. ^dGlass transition temperature and melting temperature were obtained from DSC during the second heating. $T_{\rm g,M}$ is the glass transition temperature of the PMVL domain, and $T_{\rm g,L}$ is for the PLLA domain. ^ePLLA crystallinity (%) calculated based on the area of the melting and cold crystallization peaks measured by DSC using 93.0 J/g as the enthalpy of fusion for PLLA crystals and normalized by the weight fraction of PLLA. ¹⁰ ^fPLLA melting temperature.

prepare mechanically tunable thermoplastics with excellent processability. To our knowledge, this specific design has not previously been explored for use as thermoplastic materials. We sought to prepare commercially relevant sustainable materials by using inexpensive and renewable feedstocks and scalable synthetic processes. We synthesized a series of sustainable HPMC-graft block polymers, hereafter referred to as HPMC-g-(PMVL-b-PLLA) via a simple two-step ring-opening transesterification polymerization (ROTEP) (Scheme 1). Whereas hydroxypropyl methylcellulose (HPMC) and lactide are already commercially available, MVL shows promise as a scalable and inexpensive monomer. This provides a simple yet robust platform to explore fundamental structure—property relationships for this intriguing class of materials.

As shown in Scheme 1, the dangling diblock copolymers contain a terminal crystallizable PLLA block connected to the semiflexible HPMC backbone with a rubbery PMVL bridge. PMVL and PLLA are sufficiently incompatible for the two polymers to microphase separate under certain circumstances. In the melt state, this microphase separation can occur within a range of compositions provided the molar mass is above a critical value. Even for samples where the disparate segments are expected to be miscible, crystallization of the PLLA segments can induce microphase separation. Regardless of the

proximal cause of this separation, the nanoscopic structures formed act as reversible physical cross-links. ^{6,27} The HPMC backbone acts to permanently connect the resulting microphase-separated domains much like the bridging effect that occurs with segregated domains in a linear multiblock copolymer. The potential processing and mechanical property advantages associated with this HPMC-g-(PMVL-b-PLLA) graft block molecular architecture were explored using dynamic mechanical spectroscopy (DMS) and tensile testing, respectively.

The graft block polymers studied in this work (detailed in Table 1) were prepared using a "grafting from" approach. 28,29 Two different hydroxypropyl methylcellulose polymers denoted HPMC15 ($M_{\rm n}=15\,400~{\rm kg/mol}$, D=1.84) and HPMC40 ($M_{\rm n}=39\,700~{\rm kg/mol}$, D=1.86) were used as the graft polymer backbone. Both HPMC polymers have, on average, about one unsubstituted hydroxyl group for each sugar moiety. Typically, for reactions with cellulose derivatives, organic solvents or ionic liquids are required to dissolve the materials. Onveniently, both hydroxypropyl methylcellulose compounds are soluble in the MVL monomer at 80 °C. The bulk polymerization reaches equilibrium (about 80% conversion) after a few hours at 80 °C.

Using Sn(Oct)₂ as a catalyst, we synthesized several HPMC-g-(PMVL-b-PLLA) graft block polymers from HPMC-g-PMVL.

ACS Macro Letters Letter

The compositions of the diblock grafts were controlled by adjusting the ratio of L-lactide monomer to HPMC-g-PMVL macroinitiator. Graft block polymers were prepared with PLLA volume fractions ranging from 0.3 to 0.7. In addition, we prepared a linear triblock copolymer, PLLA-b-PMVL-b-PLLA (LML (26, 0.3)), to act as a control when probing the thermodynamic and physical properties of the graft block copolymers (Figure S4, Table 1).

The HPMC-g-PMVL and HPMC-g-(PMVL-b-PLLA) polymers were characterized by ¹H NMR and size-exclusion chromatography (SEC) (Figures S1, S2, and S3 and Table S3). For HPMC15-g-PMVL and HPMC40-g-PMVL, the molar mass of the individual PMVL grafts were similar (8.5 and 8.1 kg/mol, respectively) as determined by ¹H NMR end group analysis. As shown in Figure S2 and Table 1, the overall molar mass of the graft polymers increased with PLLA content for HPMC15 (8.5, 0.3) and HPMC15 (8.5, 0.5), where the first and second numbers in the parentheses refer to the PMVL molecular weight and PLLA volume fraction, respectively. However, the two highest molecular weight samples, HPMC15 (8.5, 0.7) and HPMC40 (8.1, 0.7), could not be passed through the SEC columns. We believe the combined effects of the rigid backbone and high molecular weights grafts cause the polymer to adopt a stretched conformation and aggregate in solution.

The thermal properties of the HPMC-graft block polymers were studied using differential scanning calorimetry (DSC) (Figures 1 and S5). As shown in Figure S5, HPMC shows no

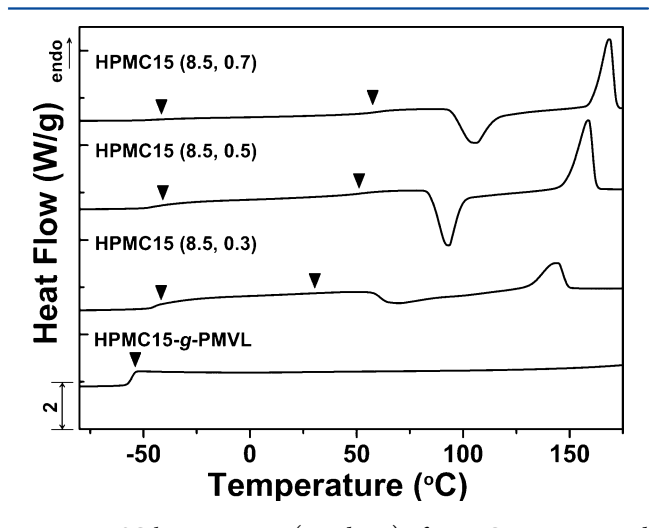


Figure 1. DSC heating curves (exo down) of HPMC15-g-PMVL and HPMC15-g-(PMVL-b-PLLA). Arrows indicate $T_{\rm g}$ values of PMVL and PLLA domains ($T_{\rm g,PMVL}$ and $T_{\rm g,PLLA}$). The second heating curves with a heating rate of 10 °C/min in DSC were used for all analyses.

thermal transitions during heating from -80 to $175\,^{\circ}\mathrm{C}.$ However, HPMC-g-PMVL (Figure 1) exhibits a glass transition temperature near $-53\,^{\circ}\mathrm{C},$ which is close to the value reported for high molar mass linear PMVL homopolymer ($T_{\mathrm{g}}=-51\,^{\circ}\mathrm{C}).^{7}$ For HPMC-graft block polymers, two distinct T_{g} values are observed, indicative of microphase separation of the PMVL and PLLA domains. The lower T_{g} value is elevated slightly in the HPMC-graft block polymers, suggesting partial incorporation of PLLA in domains that are predominately PMVL.

When designing new semicrystalline polymeric materials, it is critically important to understand the influence of molecular architecture on crystallization and the manner in which crystallinity affects material properties. Although crystallization is often desired for optimal mechanical and thermal properties, ³¹ crystallization of the PLLA homopolymer is relatively slow and can be further retarded when introduced into linear multiblock architectures. ¹⁰ It is also well established that crystallization can have a profound impact on microphase separation and the final morphology. Whereas crystallization can induce microphase separation in disordered systems, morphologies of ordered block polymers can be destroyed by breakout crystallization. ^{27,32–34} For each of the HPMC graft–block polymers, PLLA crystallization and melting peaks are both observed in the second DSC heating curve (Figure 1). Wide-angle X-ray scattering (WAXS) patterns obtained at different temperatures provide further evidence for crystallization of the HPMC-graft polymers (Figure S6).

The DSC melting profile of the PLLA blocks in HPMC-g-(PMVL-b-PLLA) is qualitatively similar to that of a linear LML triblock polymer (Figure SS) of moderate molar mass. In contrast, linear PLLA-based multiblock copolymers are often nearly (or completely) amorphous due to the confinement of the crystallizable blocks. The PLLA blocks of HPMC-g-(PMVL-b-PLLA), however, are mobile as they are tethered only on one side to the HPMC backbone. As a result, the PLLA segments comprising the graft block architecture are capable of faster crystallization than PLLA segments within a linear multiblock. As summarized in Table 1, the PLLA blocks of HPMC-graft polymers have a crystallinity of about 10%, which is approximately half that of the linear LML triblock copolymer containing PLLA blocks of comparable molar mass.

Previous reports demonstrated that cellulose-graft poly(L-lactide) or poly(ε -caprolactone) had lower crystallinity and reduced crystallization rates compared to the linear homopolymer. The obtained 14% crystallinity in HPMC40-g-PLLA, intermediate to HPMC-g-(PMVL-b-PLLA) and LML (see Figure S5). It is currently unclear whether the PLLA in the graft block polymers has a reduced extent of crystallization compared to that in the triblock polymer due to a lower rate of crystallization, or whether the graft architecture fundamentally limits the maximum crystallinity of PLLA blocks. However, the melting temperature increases with PLLA content in HPMC-graft block polymers, which suggests that the crystallization may be tuned to some extent by altering graft molar mass. We intend to further explore the nucleation and growth kinetics of these interesting materials in a subsequent study.

To explore the influence of the graft architecture on processability, we investigated the rheological properties of the HMPC-graft block polymers in the melt state at 170 °C, a temperature that is well below the degradation temperature of the samples.⁷ As shown in Figure 2A, the three HPMC-g-(PMVL-b-PLLA) graft block polymers exhibit two distinct types of rheological behavior depending on the molar mass of the PLLA blocks. At 170 °C, HPMC15 (8.5, 0.3) shows liquid-like behavior as evidenced by $G' \sim \omega^2$ and $G'' \sim \omega^1$ in the low-frequency regime.³⁷

Increasing the PLLA content to 0.5, HPMC15 (8.5, 0.5) shifts the terminal region to lower frequency but without disrupting the liquid-like behavior. Further increasing the PLLA fraction to 0.7, HPMC15 (8.5, 0.7) produces a qualitatively different result at low frequencies, including an increase in the magnitude of the dynamic elastic and loss moduli and nonterminal scaling ($G'' \sim \omega^{1/3}$, $G' \sim \omega^{1/3}$). These effects are also apparent in the frequency dependence of the dynamic viscosity as shown in Figure 2B. Both HPMC15 (8.5, 0.3) and HPMC15 (8.5, 0.5) exhibit an approach to a frequency-

ACS Macro Letters

Letter

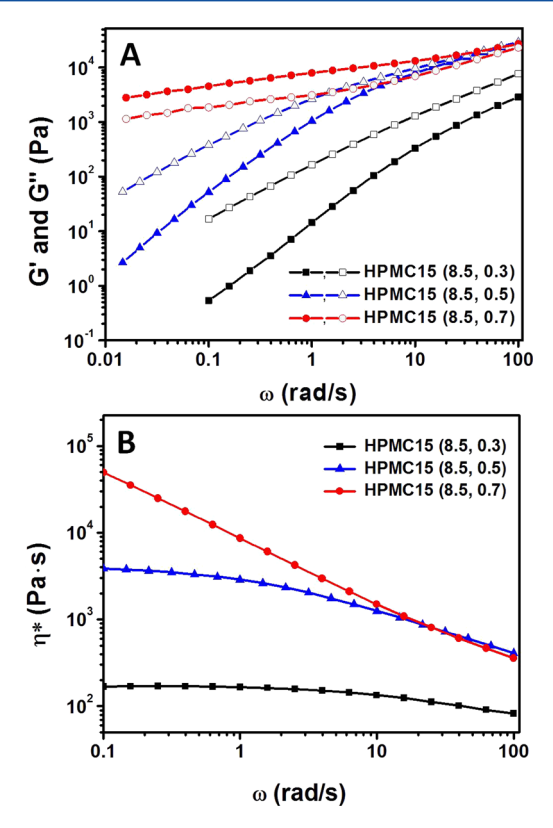


Figure 2. Linear dynamic mechanical properties of the HPMC-graft polymers determined at 170 °C: (A) storage modulus G' (filled symbols) and loss modulus G'' (open symbols); (B) complex viscosity.

independent zero-shear viscosity at low frequency that is strongly composition dependent, while HPMC15 (8.5, 0.7) displays a shear thinning (power law) response at all measurement frequencies. These trends are consistent with a state of disorder in HPMC15 (8.5, 0.3) and HPMC15 (8.5, 0.5) and microphase separation in HPMC15 (8.5, 0.7) at 170 °C. Small-angle X-ray scattering (SAXS) measurements reinforce these interpretations and reveal a state of microphase separation in all specimens following PLLA crystallization. Although the scattering data lack higher-order peaks, the primary reflection was used to estimate the domain period, 20—30 nm for the samples analyzed (see Figure S7).

On the basis of previous work, we estimate that the Flory–Huggins segment–segment interaction parameter, χ , for PLLA and PMVL is approximately 0.029 at 170 °C.³⁸ Self-consistent mean-field theory, which anticipates $(\chi N)_{\rm ODT}=10.5$ for compositionally symmetric $(f_{\rm L}=1/2)$ diblocks, predicts that the critical molar mass for a linear PMVL–PLA to microphase separate is 29 kg/mol at 170 °C. Notably, this is higher than the molar mass (18 kg/mol) of the diblock grafts in HPMC15 (8.5, 0.5). We are unaware of an existing theoretical translation of this diblock prediction to the graft block copolymer architecture but note that linking many PLLA–PMVL chains into a graft copolymer seems to preserve the gross thermodynamic characteristics embodied in the diblock. A similar trend has been demonstrated when diblocks are linked end-to-end in a linear multiblock molecular architecture.³⁹

The mechanical properties of all graft polymers were characterized using uniaxial tensile tests. Representative engineering stress versus strain data for each sample are plotted in Figure 3A. Average values of the mechanical properties (determined with at least five samples) including elastic modulus (E), strain at break (ε_b) , stress at break (σ_b) , yield strength (σ_y) , and tensile toughness (integrated area under the stress–strain curve) are summarized in Table S1.

As shown in Figure 3A, architecture greatly influences the tensile properties of the materials. For example, while HPMC15 (8.5, 0.3) has a strain at break that is nearly double that of the linear triblock LML (26, 0.3) of similar composition, the ultimate tensile strength is reduced. HPMC15 (8.5, 0.5) retains excellent elongation at break (790%) and shows both an increased toughness and increased ultimate tensile strength as compared to the triblock or low PMVL composition sample. Increasing the PLLA volume fraction further transforms the material from an elastomer to a ductile plastic. Accordingly, HPMC15 (8.5, 0.7) has a lower strain at break but much higher stress at break than samples with a minority of PLLA. Introducing a longer cellulosic backbone at fixed side chain composition, HPMC40 (8.5, 0.7) versus HPMC15 (8.5, 0.7), roughly doubles the strain at break and toughness. These graft block polymers present an excellent platform for tuning the elasticity, toughness, and tensile strength of the thermoplastics by varying backbone lengths and segment compositions of the dangling blocks.

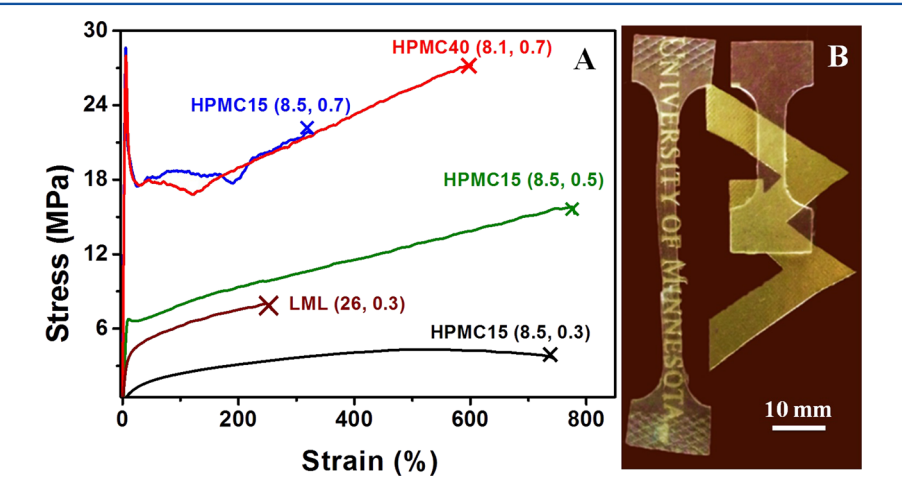


Figure 3. (A) Representative examples of room-temperature uniaxial tensile testing of selected HPMC15-grafted, HPMC40-grafted, and linear triblock copolymers. (B) Representative examples of stretched (left) and unstretched (right) samples from HPMC15 (8.5, 0.7).

ACS Macro Letters

Letter

The existence of the PMVL block in the graft polymers is essential for toughening. As shown in Figures S9 and S10, HPMC-g-PLLA with comparable graft molar mass (17 kg/mol) is hard and quite brittle with a breaking strain of only 6%. Interestingly, the plastically deformed graft-block specimens remain fully transparent and are homogeneous in appearance up to the breaking point (Figure 3B). Moreover, in the plastic limit neither HPMC15 (8.5, 0.7) nor HPMC40 (8.5, 0.7) shows a necking behavior; the entire gauge section of the tensile bars deforms uniformly. This indicates that the deformation mechanism may be different from that typically observed with rubber toughened plastics, 40,41 where stress whitening occurs coincident with yielding and necking. We speculate that the intrinsically rigid HPMC backbones effectively transfer stress between numerous adjacent PLLA crystallites mediated by the amorphous and rubbery (predominately PMVL) domains. Under stress, these graft polymers apparently are not susceptible to cavitation and crazing.⁴² More in-depth investigations about the toughening mechanisms of these HPMC-graft block polymers will be pursued in the future.

In conclusion, we have shown that a diblock graft architecture containing rubbery interior and semicrystalline exterior blocks tethered to a semiflexible backbone can be used to create thermoplastics with superior and tunable mechanical and rheological properties. These materials were constructed using renewable and potentially inexpensive feedstocks, HPMC, MVL, and L-lactide. Placement of the semicrystalline block at the end of the grafted chains affords crystallinity that is not readily attainable using a linear multiblock molecular architecture. Remarkably, these commercially promising tough graft block HPMC thermoplastics deform plastically without necking and remain transparent when strained as much as 600% prior to failure.

ASSOCIATED CONTENT

S Supporting Information

The Supporting Information is available free of charge on the ACS Publications website at DOI: 10.1021/acsmacrolett.6b00091.

Experimental details and additional characterization data (Figures S1- S10, Table S1, S2) (PDF)

AUTHOR INFORMATION

Corresponding Author

*E-mail: bates001@umn.edu.

Notes

The authors declare no competing financial interest.

ACKNOWLEDGMENTS

Funding for this work was provided by the Center for Sustainable Polymers at the University of Minnesota, a National Science Foundation (NSF)-supported Center for Chemical Innovation (CHE-1413862). SAXS data were at the DuPont-Northwestern Dow Collaborative Access Team (DND-CAT) Synchrotron Research Center located at Sector 5 of the APS. DND-CAT is supported by the E.I. DuPont de Nemours & Co., The Dow Chemical Company, the U.S. National Science Foundation through Grant DMR-9304725, and the State of Illinois through the Department of Commerce and the Board of Higher Education Grant IBHE HECA NWU 96. Use of the APS was supported by the U.S. Department of

Energy, Office of Science, Office of Basic Energy Sciences, under Contract No. DE-AC02-06CH11357.

REFERENCES

- (1) Yu, L.; Dean, K.; Li, L. Prog. Polym. Sci. 2006, 31, 576-602.
- (2) Legge, N. R. Rubber Chem. Technol. 1987, 60, 83-117.
- (3) Pinchuk, L.; Wilson, G. J.; Barry, J. J.; Schoephoerster, R. T.; Parel, J. M.; Kennedy, J. P. *Biomaterials* **2008**, 29, 448–460.
- (4) Reneker, D. H.; Chun, I. Nanotechnology 1996, 7, 216-223.
- (5) Bates, F. S.; Hillmyer, M. A.; Lodge, T. P.; Bates, C. M.; Delaney, K. T.; Fredrickson, G. H. *Science* **2012**, *336*, 434–440.
- (6) Koo, C. M.; Wu, L. F.; Lim, L. S.; Mahanthappa, M. K.; Hillmyer, M. A.; Bates, F. S. *Macromolecules* **2005**, *38*, 6090–6098.
- (7) Xiong, M. Y.; Schneiderman, D. K.; Bates, F. S.; Hillmyer, M. A.; Zhang, K. C. *Proc. Natl. Acad. Sci. U. S. A.* **2014**, *111*, 8357–8362.
- (8) Wang, S.; Kesava, S. V.; Gomez, E. D.; Robertson, M. L. *Macromolecules* **2013**, *46*, 7202–7212.
- (9) Matsen, M. W. Macromolecules 2012, 45, 2161-2165.
- (10) Panthani, T. R.; Bates, F. S. Macromolecules 2015, 48, 4529-4540.
- (11) Hillmyer, M. A.; Tolman, W. B. Acc. Chem. Res. **2014**, 47, 2390–2396.
- (12) Martello, M. T.; Schneiderman, D. K.; Hillmyer, M. A. ACS Sustainable Chem. Eng. 2014, 2, 2519–2526.
- (13) Lee, I.; Panthani, T. R.; Bates, F. S. Macromolecules 2013, 46, 7387-7398.
- (14) Schindler, A.; Harper, D. J. Polym. Sci., Polym. Chem. Ed. 1979, 17, 2593-2599.
- (15) Ukielski, R. Polymer 2000, 41, 1893-1904.
- (16) Zhao, C. Z.; Wu, D. X.; Huang, N.; Zhao, H. Y. J. Polym. Sci., Part B: Polym. Phys. 2008, 46, 589-598.
- (17) Goodwin, A.; Wang, W.; Kang, N.-G.; Wang, Y.; Hong, K.; Mays, J. Ind. Eng. Chem. Res. 2015, 54, 9566–9576.
- (18) Ruzette, A. V.; Leibler, L. Nat. Mater. 2005, 4, 19-31.
- (19) Shim, J. S.; Kennedy, J. P. J. Polym. Sci., Part A: Polym. Chem. 1999, 37, 815–824.
- (20) Weidisch, R.; Gido, S. P.; Uhrig, D.; Iatrou, H.; Mays, J.; Hadjichristidis, N. *Macromolecules* **2001**, *34*, 6333–6337.
- (21) Hadjichristidis, N.; Xenidou, M.; Iatrou, H.; Pitsikalis, M.; Poulos, Y.; Avgeropoulos, A.; Sioula, S.; Paraskeva, S.; Velis, G.; Lohse, D. J.; Schulz, D. N.; Fetters, L. J.; Wright, P. J.; Mendelson, R. A.; Garcia-Franco, C. A.; Sun, T.; Ruff, C. J. *Macromolecules* **2000**, 33, 2424–2436.
- (22) Lin, Y.; Wang, Y.; Zheng, J.; Yao, K.; Tan, H.; Wang, Y.; Tang, C.; Xu, D. *Macromolecules* **2015**, *48*, 7640–7648.
- (23) Onishi, Y.; Eshita, Y.; Murashita, A.; Mizuno, M.; Yoshida, J. J. Appl. Polym. Sci. 2005, 98, 9–14.
- (24) Jiang, F.; Wang, Z. K.; Qiao, Y.; Wang, Z. G.; Tang, C. B. *Macromolecules* **2013**, *46*, 4772–4780.
- (25) Liu, Y. P.; Yao, K. J.; Chen, X. M.; Wang, J. F.; Wang, Z. K.; Ploehn, H. J.; Wang, C. P.; Chu, F. X.; Tang, C. B. *Polym. Chem.* **2014**, 5, 3170–3181.
- (26) Yan, C. H.; Zhang, J. M.; Lv, Y. X.; Yu, J.; Wu, J.; Zhang, J.; He, J. S. Biomacromolecules **2009**, 10, 2013–2018.
- (27) Quiram, D. J.; Register, R. A.; Marchand, G. R. Macromolecules 1997, 30, 4551–4558.
- (28) Hadjichristidis, N.; Pitsikalis, M.; Iatrou, H.; Driva, P.; Chatzichristidi, M.; Sakellariou, G.; Lohse, D. In *Encyclopedia of Polymer Science and Technology*; John Wiley & Sons, Inc.: New York, 2002.
- (29) Duan, Y. X.; Thunga, M.; Schlegel, R.; Schneider, K.; Rettler, E.; Weidisch, R.; Siesler, H. W.; Stamm, M.; Mays, J. W.; Hadjichristidis, N. *Macromolecules* **2009**, 42, 4155–4164.
- (30) Roy, D.; Semsarilar, M.; Guthrie, J. T.; Perrier, S. Chem. Soc. Rev. **2009**, 38, 2046–2064.
- (31) Garlotta, D. J. Polym. Environ. 2001, 9, 63-84.
- (32) Koo, C. M.; Hillmyer, M. A.; Bates, F. S. Macromolecules 2006, 39, 667-677.

ACS Macro Letters

Letter

(33) Bishop, J. P.; Register, R. A. Macromolecules 2010, 43, 4954–4960.

- (34) Nandan, B.; Hsu, J. Y.; Chen, H. L. J. Macromol. Sci., Polym. Rev. **2006**, 46, 143–172.
- (35) Yuan, W. Z.; Yuan, J. Y.; Zhang, F. B.; Xie, X. M. Biomacromolecules 2007, 8, 1101–1108.
- (36) Carlmark, A.; Larsson, E.; Malmstrom, E. Eur. Polym. J. 2012, 48, 1646-1659.
- (37) John, M. D.; Ronald, G. L. In Structure and Rheology of Molten Polymers; Carl Hanser Verlag GmbH & Co. KG: 2006; pp 91–130.
- (38) Schneiderman, D. K.; Hillmyer, M. A. Macromolecules 2016, DOI: 10.1021/acs.macromol.6b00211.
- (39) Wu, L. F.; Cochran, E. W.; Lodge, T. P.; Bates, F. S. *Macromolecules* **2004**, *37*, 3360–3368.
- (40) Bartczak, Z.; Galeski, A. In *In Polymer Blends Handbook*; Springer: 2014; pp 1203–1297.
- (41) Li, T.; Heinzer, M. J.; Francis, L. F.; Bates, F. S. J. Polym. Sci., Part B: Polym. Phys. **2016**, 54, 189–204.
- (42) Leibler, L. Prog. Polym. Sci. 2005, 30, 898-914.